

Experimental Studies on Seismic Behavior of Reinforced Concrete Members of High-Strength Concrete

by S. Sugano, T. Nagashima, H. Kimura,
A. Tamura, and A. Ichikawa

Synopsis: Three earthquake type loading tests of reinforced concrete (R/C) columns, short beams and beam-column joints using high strength concrete were carried out. The main objectives of this program were to investigate the seismic behavior of R/C members using high strength concrete, and to obtain guidelines for their design for high-rise buildings. Concretes having three levels of compressive strength, 400, 600 and 800kg/cm² (39, 59 and 78 MPa) were used. High strength reinforcing bars with nominal yield strengths of 8500 and 14000kg/cm² (834 and 1370 MPa) were provided for lateral reinforcement. Longitudinal reinforcement with a yield strength of 6000kg/cm² (588 MPa) was also used for beam-column joint test. Emphasis was put on the combination of high strength concrete and high strength reinforcing bars. The seismic behavior of columns, short beams and beam-column joints under high axial load, high beam shear and high joint shear, respectively, were observed. The relationship between ductility and amount of lateral reinforcement were particularly discussed in the column and short beam tests. In beam-column joint test, several joint details were considered and their behavior was investigated. The design guidelines for these high strength concrete members were also presented in this paper. The results of this experimental program show that the combination of high strength concrete and high strength steel bars can be quite effective in improving strength and ductility of R/C members of high-rise buildings.

Keywords: beams (supports); columns (supports); ductility; earthquake resistant structures; high-rise buildings; high-strength concretes; high-strength steels; joints (junctions); lateral pressure; reinforced concrete; research; tests

S. Sugano, Dr. is a chief research engineer of the Technical Research Laboratory at TAKENAKA Corporation, Tokyo, Japan. He has performed extensive research works on reinforced concrete structures, and is active in both the J.C.I. and A.I.J.

T. Nagashima is a chief research engineer of the Technical Research Laboratory at TAKENAKA Corporation, Tokyo, Japan. His current research interests include, design and analysis of high rise R/C structures and high-strength structural materials.

H. Kimura is a research engineer of the Technical Research Laboratory at TAKENAKA Corporation, Tokyo, Japan. His research field includes experimental and analytical studies on R/C high rise buildings and experimental studies on R/C members using high-strength concrete.

A. Tamura is a staff of the Building Structural Design Department in Tokyo Main Office at TAKENAKA Corporation, Tokyo, Japan. His current interests include design of high rise R/C structures.

A. Ichikawa is a research engineer of the Technical Research Laboratory at TAKENAKA Corporation, Tokyo, Japan. His recent research covers design and analysis of R/C high rise buildings and experimental studies on high-strength concrete members.

INTRODUCTION

During the 1980's, the number of tall reinforced concrete framed buildings of 30 stories or higher has been increasing in Japan [Refs. 1,2]. These structures utilize concretes with specified strengths (f_c) up to 480kg/cm^2 (47 MPa), relatively small member sections, and larger and higher yield strength reinforcing bars. Furthermore, the need to build higher R/C structures, to widen column spans and to reduce member sizes has arisen and is widely recognized among structural engineers and researchers. To make these things possible, the utilization of higher strength materials, (such as high-strength concrete with a compressive strength of 500kg/cm^2 (49 MPa) or higher, high-strength main bars with yield strength of 5000kg/cm^2 (490 MPa) or higher) is needed. The authors of this paper have been studying R/C members composed of high-strength materials [Refs. 3, 4, 5, 6]. However, there is currently no available code covering R/C

structures using such high strength materials. In addition, knowledge on the structural behavior of R/C members and structures utilizing high-strength materials is limited. This paper presents empirical results of tests on a prototype column, a short span beam and a beam-column joint made with high strength concrete ($f_c=600 \sim 800 \text{ kg/cm}^2$; $59 \sim 78 \text{ MPa}$) and high strength reinforcing bars. Emphasis was put on the combination of high and ultra-high strength reinforcing bars so as to effectively confine the high strength, relatively more brittle concrete. The main objectives of these three tests were to determine the seismic behavior of high strength concrete members and to obtain guidelines for their design for very tall buildings.

COLUMN TEST

Test Specimen

Eight column specimens were tested under earthquake-type loadings. The cross section ($25 \times 25 \text{ cm}$), area ratio of longitudinal reinforcement (2.4 %) and shear span ratio (2.0), were common to all the specimens, as shown in Fig.1 . The variables were :

1)specified compressive strengths of concrete (f_c) with 400, 600 and 800 kg/cm^2 (39, 59 and 78 MPa) ;

2)full capacity of lateral reinforcement ($P_w \cdot f_{y, n}$), where P_w and $f_{y, n}$ are area ratio of lateral reinforcement and yield strength of steel bar ; and

3)the ratio of axial stress to specified compressive strength of concrete (0.3 and 0.55) .

Table 1 gives variables for each specimen and the nominal shear stresses ($v_{m, u}$) calculated from the flexural strengths of the columns. The flexural strengths of the columns (M_u) were determined by the following Abe's empirical equations (1) [Ref. 7].

$$M_u = \xi_{\kappa} \cdot F_{\kappa} \cdot D \quad (\text{kg} \cdot \text{cm}) \quad (1)$$

where :

$$\xi_{\kappa} = A_p \{ \tanh(B_p(1 - \eta_{\gamma})) - 0.5(1 - \eta_{\gamma}) \}$$

$$A_p = 0.315 \cdot R_s + 0.424 \quad , \quad B_p = 0.362 \cdot R_f + 0.948$$

$$\eta_{\gamma} = N / F_{\kappa} \quad , \quad R_s = T_o / C_o \quad , \quad R_f = C_o / T_o$$

$$F_{\kappa} = C_o (N + T_o) / (C_o + 2T_o) + T_o$$

$$C_o = f_c' \cdot b \cdot D, \quad T_o = f_y \cdot a_{\kappa}$$

f_c' : Concrete strength (kg/cm²),
 b : Column width (cm),
 D : Column depth (cm),
 f_y : Yield strength of main bar (kg/cm²),
 a_s : Total area of longitudinal reinforcement (cm²)
 N : Axial force (kg)

Original application ranges of variables in equation (1) are as follows.

$a_s/(b \cdot D)$: 0.7~4.0 %
 f_c' : 200~300 kg/cm² (20~ 29 MPa)
 f_y : 3000 ~4500 kg/cm² (294~441 MPa)
 N : All range from tensile strength to compressive strength of the section.

The full capacities of lateral reinforcement of the specimens 1, 2, 3, 5, and 7 were determined so as to be approximately equal to the nominal shear stresses attained in the specimens. Specimen 4 had a capacity of lateral reinforcement almost half of the nominal shear stress, while specimens 6 and 8 had 1.5 times as much full capacity of lateral reinforcement as nominal shear stress. The mechanical characteristics of concretes and reinforcing bars are shown in Table 2 and 3. Lateral reinforcement was arranged so as to restrain each longitudinal reinforcement against buckling, as shown in Fig. 1. It should be noted that all hoop steel of both deformed bars and high strength bars was butt-welded. For ultra-high strength bars, outer(perimeter) square spiral hoops and inner hoops with 135° bends extending for 8 bar diameters were provided.

Reversed cyclic horizontal load was applied to each specimen while the axial load was held constant. The inflection point was kept at midheight of the column by using loading apparatus for the test, as shown in Fig. 2.

Test Results and Discussions

Table 4 gives the main test results. Fig.3 and 4 show a comparison of measured horizontal load-interstory loops and the envelopes of horizontal load-interstory relations. Specimens 1 and 2 with $f_c=600$ and 800 kg/cm² (59 and 78 MPa) concretes, respectively, tested under the lower ratio of axial stress to specified compressive strength of concrete (0.3), and exhibited excellent ductility, the energy dissipating capability and the lateral load carrying capacity up to the interstory drift exceeding 5 % . On the other hand, all other specimens, tested under the higher axial compressive stress of 55 % of the specified concrete strength, behaved in less ductile manner when compared with specimens 1 and 2.

The failure mode for specimens 1 and 2 was flexural failure, and for all other specimens it was flexural compression failure. Specimens 3, 5, and 7, had almost the same ratio of the amount of lateral reinforcement to the nominal shear stress of the column ($P_w \cdot f_n / v_{max} = 1.0$) and the same ratio of axial stress to the specified concrete strength (0.35), but different specified concrete strengths with 400, 600 and 800 kg/cm² (39, 59 and 78 MPa), respectively. These specimens had almost the same ultimate displacement (R_u , approximately 2 %) at which 80 % of the maximum lateral load was sustained. Comparing specimens 4, 5 and 6 having the same concrete strength ($f_c = 600$ kg/cm²; 59 MPa) but different amount of lateral reinforcement, the displacement ductility increased in proportion to the full capacity of lateral reinforcement. The same effect was also observed in comparison between specimens 7 and 8 ($f_c = 800$ kg/cm²; 78 MPa).

The measured maximum strength in each specimen was larger than the calculated flexural strength using Abe's empirical equation (1) and the following equations (2a~ 2c) proposed by A. I. J. [Ref. 8], particularly in the specimens tested under the higher axial force.

In case : $N_{max} \geq N > N_b$

$$M_u = \{0.5a_s \cdot f_y \cdot g_i \cdot D + 0.024(1+g_i)(3.6-g_i)b \cdot D^2 \cdot f_c'\} \left(\frac{N_{max} - N}{N_{max} - N_b} \right) \quad (\text{kg} \cdot \text{cm}) \quad (2a)$$

In case : $N_b \geq N \geq 0$

$$M_u = 0.5a_s \cdot f_y \cdot g_i \cdot D + 0.5N \cdot D \left(1 - \frac{N}{b \cdot D \cdot f_c'} \right) \quad (\text{kg} \cdot \text{cm}) \quad (2b)$$

In case : $0 > N \geq N_{min}$

$$M_u = 0.5a_s \cdot f_y \cdot g_i \cdot D + 0.5N \cdot g_i \cdot D \quad (\text{kg} \cdot \text{cm}) \quad (2c)$$

$$\begin{aligned} \text{where : } N_{max} &= b \cdot D \cdot f_c' + a_s \cdot f_y \\ N_b &= 0.22(1+g_i)b \cdot D \cdot f_c' \\ N_{min} &= -a_s \cdot f_y \end{aligned}$$

g_i is the ratio of the distance between tension and compression reinforcements gravity center to the column depth. Other notations in equation (2a~ 2c) are the same as those in equation (1).

The relationship between the amount of lateral reinforcement normalized by measured concrete strength ($P_w \cdot f_n / f_c'$) and the ultimate drift (R_u) is shown in Fig. 5. The ultimate drift increased in proportion to the amount of lateral reinforcement for both of $f_c = 600$ and 800 kg/cm² (59

and 78 MPa) concretes test specimens. To obtain the ductility up to the displacement level of 2 % under the high axial compression stress of about 60 % of the concrete strength, the full capacity of lateral reinforcement normalized by concrete strength ($P_w \cdot f_{y,h} / f_c'$) must be greater than 0.10 .

SHORT SPAN BEAM TEST

Test Specimen

Ten short span beam specimens with 20×30 cm cross section, as shown in Fig.6, were tested under seismic-type loadings. The shear span ratio was 1.5 for all specimens. Variables were :

1) specified compressive strength of the concrete (f_c) with 400, 600 and 800 kg/cm² (39, 59 and 78 MPa) ;

2) nominal shear stress levels of beams at hinging mechanism ($v_{m,u}$) with approximately 40 and 60 kg/cm² (3.9 and 5.2 MPa); and

3) full capacity of lateral reinforcement $P_w \cdot f_{y,h}$ ($P_w \cdot f_{y,h} / v_{m,u} \cong 0.5, 1.0, 1.5$), where P_w and $f_{y,h}$ are area ratio of lateral reinforcement and yield strength of steel bar.

Details of these specimens are shown in Table 5. The full capacity of lateral reinforcement of the specimens 1, 4, 6, 8 and 10 were established to be approximately equal to the nominal shear stresses ($v_{m,u}$) attained in the specimens at the plastic hinge location. Specimens 3 and 9 had the lateral reinforcement with a capacity of almost half of the nominal shear stress, while specimens 2, 5 and 7 had 1.5 times as much full capacity of lateral reinforcement as the nominal shear stress. Mechanical characteristics of steel bars are given in Table 6. All lateral reinforcements of both deformed bars and high strength bars were butt-welded. For ultra-high strength bars, double square spiral stirrups were provided. The specimens were positioned in the testing frame and were subjected reversed cyclic load, as shown in Fig.7.

Test Results and Discussions

Table 7 gives the relevant test results. Fig.8 shows the relationship between the shear force and deflection (relative displacement of both end of the beam). Comparison of the envelopes of shear force-deflection curves are indicated in Fig.9 .

All specimens exhibited flexural yielding at a displacement angle of approximately 1 % and three different failure modes, specifically shear failure at the hinge zone, shear-diagonal tension failure, and bond splitting failure were observed at larger drift levels. Except for specimens 3 and 9, whose full capacity of lateral reinforcement were almost half of the nominal shear stress, the shear force - deflection curves gradually decreased at displacement angles larger than 4 % because the shear cracks at the hinge zone were spreading and the concrete was broken into pieces. The failure mode for these specimens was a shear failure at the hinge zone after yielding.

Specimen 3 with shear stress level v_{mu} of 60 kg/cm² (5.9 MPa) and full capacity of lateral reinforcement of half of v_{mu} , dropped its load at a displacement angle 3.5 % because of shear-diagonal tension failure after flexural yielding. Specimen 9 with shear stress level v_{mu} of 40 kg/cm² (3.9 MPa) and full capacity of lateral reinforcement of half of v_{mu} , showed bond splitting failure after flexural yielding. Except for specimens 3 and 9, the relationship between shear force and displacement of specimens with shear stress levels of 60 and 40 kg/cm² (5.9 and 3.9 MPa) showed a little pinching shape but performed well up to the displacement angle 4 % and 5 %, respectively. In specimens 3 and 9, the relationship between shear force-deflection was pinched after yielding of main bars and the load drop in second cycle at displacement angle 2~3 % was significant.

All measured maximum strengths were evaluated by the theory for flexural strength using idealized exponential function stress-strain relationship for concrete and/or the following equation (3) of AIJ code [Ref.9].

$$M_u = 0.9a_s \cdot f_y \cdot d \quad (\text{kg} \cdot \text{cm}) \quad (3)$$

in which

- a_s : Total area of tension reinforcing bars (cm²)
- f_y : Yield strength of tension reinforcing bars (kg/cm²)
- d : Effective beam depth (cm)

In the specimens with full capacity of lateral reinforcement equal to or larger than v_{mu} , the ultimate displacement angle (R_u) at which 80 % of the maximum force was sustained did not increase as the full capacity of lateral reinforcement and/or the compressive strength of concrete increased. This phenomenon is different from that observed in column test. The values of R_u were approximately 5 % at v_{mu} level of 60 kg/cm² (5.9 MPa) and approximately 6 % at v_{mu} level of 40 kg/cm² (3.9 MPa), respectively.

BEAM-COLUMN JOINT TEST

Test Specimens

Simulated earthquake load test on eight half-scale interior beam-column subassemblages shown in Fig.10 were performed. Details of specimens are given in Table 8. The main variables were :

- 1) specified compressive strength of the concrete (f_c) with 400, 600 and 800 kg/cm² (39, 59 and 78 MPa) ;
- 2) joint shear stress (v_j) levels of 140, 170 and 200 kg/cm² (13.7, 16.7 and 19.6 MPa) ; and
- 3) details of joint.

Fig.12 illustrates details for each joint. Four types of joint detail were considered. These were, reinforcement using high strength bars (J4-0, J6-0, J8-0, J8H-0), anchor plates attached to beam bars within the joint to prevent bar slippage (J6-1), relocation of beam plastic hinges away from the joint (J6-2) and reinforcement using steel plates (J6-3, J8H-3). The J6-2 beam main bars through the joint, were ultra-high-strength bars with a yield strength of 10600 kg/cm² (1040 MPa) and were spliced to normal strength bars using a screw sleeve, 200 mm away from the column faces, in order to relocate the beam hinges. It should be noted that all the hoops and stirrups associated with high-strength bars with yield strength of about 9000 kg/cm² (883 MPa), were butt-welded. The beam and column main bars of the J8H series were high-strength bars having a yield strength of 6000 kg/cm² (588 MPa). The ratio of joint depth to beam bar diameter was 20.0 in all the specimens. All specimens except for J6-2, were designed so as to form plastic hinges in the beams adjacent to the column faces. All specimens had a transverse beam on one side. The mechanical characteristics of the concretes and reinforcing bars are shown in Table 9. The test system is illustrated in Fig.11. Reversed cyclic loads were applied at the beam tips, while the column axial load was held constant (at 200t) during the test.

Test Results and Discussions

Fig.13 shows the relationships between story shear and story drift. Only specimen J4-0 with $f_c=400$ kg/cm² (39 MPa) concrete failed in joint shear before flexural yielding of the beam and showed a considerable deterioration in load carrying capacity during the test. The maximum story shear of J4-0 was 15 % smaller than those from specimens J6-0 and J8-0 with concrete strengths of 600 and 800 kg/cm² (59 and

78 MPa), respectively. J6-0 and J8-0 formed beam hinges, and showed a stable story shear-story drift relationship up to 5 % of the story drift, but failed in joint shear at a drift larger than 5 %. Specimen J6-1 with anchor plates attached to the beam bars within the joint, showed the same behavior as J6-0 since their beam main bar slippage was not significant and the anchor plates did not work effectively. Specimen J6-2 formed plastic hinges away from the column face as designed, and behaved in a very ductile manner until the loading was terminated at 5 % of story drift due to the torsional deformation of the beam. In comparing J6-3 to J6-0, and J8H-3 to J8H-0, the joint reinforced with steel plates showed less deterioration in the load carrying capacity than that with hoop-steel. The specimens of the J8H series utilizing high-strength beam bars, exhibited flexural beam yielding. The story shear-story drift relationship was stable up to 5 % of story drift and no significant pinching effect was observed. However, specimen J8H-0 suffered heavier damage in the joint than specimen J8-0 because the higher strength beam bars in the joint of J8H-0, produced higher shear stress.

As shown in Table 10, the measured maximum joint shear stresses in all specimens except J4-0 were larger than the calculated values, which were based on the beam flexural strength. It should be noted that the maximum shear stress was evaluated using the equation in the footnotes of Table 10. The shear cracking stress in joints in high strength concrete can be approximately evaluated by using an empirical equation also noted in the footnotes of Table 10.

Fig. 14 shows the maximum joint shear stress versus compressive strength of concrete. The figure plots the test results from this paper and other test data, including high strength concrete of over 360 kg/cm² (35 MPa). The broken line shows the nominal shear strength recommended in the design guideline of the A. I. J. [Ref. 10], for a concrete strength ranging from 210 to 360 kg/cm² (21 to 35 MPa). This corresponds with the test data showing the joint shear failure prior to beam hinging, and is marked with solid triangles. It should be noted that the method used to calculate the shear stress in the design guideline, is a little different from that utilized in this paper, as shown in the footnote of Fig. 14. The test results described in this paper indicate that the premature failure of a joint in shear can be prevented if the nominal shear stress in joint does not exceed $5\sqrt{f_c'}$ for high strength concretes ranging from 360 to 900 kg/cm² (35 to 88 MPa).

CONCLUDING REMARKS

The results obtained from the tests on high strength concrete members are summarized as follows.

1) The use of high or ultra-high strength steel bars in a column can effectively confine concretes with the strengths up to 800 kg/cm² (78 MPa).

2) To ensure the ductile behavior of high strength concrete columns, the full capacity of lateral reinforcement ($P_w \cdot f_{y,h}$) must be increased in proportion to the concrete strength. The full capacity of lateral reinforcement normalized by concrete strength ($P_w \cdot f_{y,h}/f_c'$) must be constant at a level of 0.10 or greater.

3) To obtain ductility of a column subjected to displacement level up to 2 % and with an axial compression stress of 60 % of concrete strength, the full capacity of lateral reinforcement normalized by concrete strength ($P_w \cdot f_{y,h}/f_c'$) must be greater than 0.10 .

4) For short span beams with full capacity of lateral reinforcement equal to or larger than nominal shear stress ($v_{m,u}$), the ultimate displacement angles (R_u) at which 80 % of the maximum force was sustained were approximately 5 % at $v_{m,u}$ level of 60 kg/cm² (5.9 MPa) and approximately 6 % at $v_{m,u}$ level of 40 kg/cm² (3.9 MPa), respectively. However, R_u did not increase as the full capacity of lateral reinforcement or the compressive strength of concrete increased.

5) Under high joint shear stress, interior beam-column subassemblages using high strength concrete with a compressive strength larger than 600 kg/cm² (59 MPa) had sufficient load carrying capacity up to a 5 % story drift.

6) Relocation of beam plastic hinges away from the joint reduced the damage of the beam-column joint. Also joint reinforcement by steel plates was effective in improving the load carrying capacity, when subject to a large story drift.

7) To prevent a premature joint shear failure, the nominal shear stress in the joint should be less than $5 \sqrt{f_c'}$ for concretes with strengths 360 to 900 kg/cm² (35 to 88 MPa).

CONVERSION FACTORS

$$\begin{aligned} 1 \text{ kgf} &= 9.80665 \text{ N} (= 2.2046 \text{ lb.}) \\ 1 \text{ kgf/cm}^2 &= 9.80665 \times 10^{-2} \text{ MPa} (= 14.2125 \text{ psi}) \\ 1 \text{ N/mm}^2 &= 1 \text{ MPa} \end{aligned}$$

REFERENCES

1. 'Proceedings of the Seminar on Reinforced Concrete High-Rise Buildings in Japan with Special Concern on Aseismic Design of Beam-Column joints'. PMFSEL Report No. 87-5, The University of Texas at Austin.
2. S.Sugano, T.Nagashima, H.Kimura, et al., "Seismic Design of a Thirty-Story Reinforced Concrete Building", Proceedings of 9th WCEE, 1988.
3. S.Sugano, T.Nagashima, H.Kimura, et al., "Experimental Studies on Seismic Behavior of High Strength Concrete Columns Laterally Reinforced with High Strength Steel Bars", Proceedings of 9th WCEE, 1988.
4. S.Sugano, T.Nagashima, H.Kimura, et al., "Experimental Studies on Seismic Behavior of High Strength Concrete Columns and Beams Laterally Reinforced with High Strength Steel Bars", Proceedings of the Japan Concrete Institute, Vol.10, 1988. (in Japanese)
5. S.Sugano, T.Nagashima, H.Kimura, et al., "Experimental Studies on Seismic Behavior of High Strength Concrete Beam-Column Joint", Proceedings of the Japan Concrete Institute, Vol.11, 1989. (in Japanese)
6. S.Sugano, T.Nagashima, H.Kimura, et al., "An Experimental Study on Behavior of Reinforced Concrete Interior Beam-Column Joints of High Strength Concrete", Proceedings of 4th National Conference on Earthquake Engineering, 1990 (to be published)
7. K.Abe, "A Proposition of Equations to Calculate Ultimate Bending Strength about the Principal and the Diagonal Axes of Reinforced Concrete Columns under All Range of Axial Force", CONCRETE JOURNAL, Vol. 23, No. 9, Sept. 1985, Japan Concrete Institute (JCI No. 240)
8. "Strength and Ductility for Seismic Resistant Design of Buildings", Architectural Institute of Japan, 1981. (in Japanese)
9. "Standard for Structural Calculation of Reinforced Concrete Structures", Architectural Institute of Japan, 1985. (in Japanese)
10. "Design Guideline for Earthquake Resistant Reinforced Concrete Buildings Based on Ultimate Strength Concept", Architectural Institute of Japan, 1988. (in Japanese)

Table 1 Details of Column Test Specimens

*1 : unit(kg/cm²)

Specimen	Axial Load Ratio	fc	v _{mu}	f _{yh}	P _w	P _w ·f _{yh}	Lateral Reinforcement
		*1	*1	*1	(%)	*1	
1	0.30	600	62.0	8490	0.70	59.4	4-5 φ @45mm
2		800	77.6	8490	0.90	76.4	4-5 φ @35
3	0.55	400	46.8	8490	0.57	48.4	4-5 φ @55
4		600	62.8	3210	1.01	32.4	4-D6 @50
5				8490	0.78	66.2	4-5 φ @40
6		800	78.4	13880	0.70	97.2	4-U5.1 φ @45
7				8490	0.90	76.4	4-5 φ @35
8		13880	0.90	124.9	4-U5.1 φ @35		

Axial load ratio : Ratio of axial stress to specified concrete strength.

fc : Specified compressive strength of concrete.

v_{mu} : Shear stress calculated by Abe's empirical equation(Ref. 1)

f_{yh} : Yield strength of lateral reinforcement.

P_w : Area ratio of lateral reinforcement.

Table 2 Mechanical Characteristics of Concretes

*1 unit(kg/cm²)

	fc *1	fc' *1	E _{1/3} fc' (10 ⁵ kg/cm ²)	ft *1
Sealed Cylinders 20cm high* 10cm dia.	400	353	3.31	27
	600	680	3.90	34
	800	861	4.19	43

fc' : Measured compressive strength of concrete

E_{1/3}fc' : Secant Modulus of concrete at fc'/3

ft : Measured splitting tensile strength

Table 3 Mechanical Characteristics of Steel Bars

Type of Steel Bars		f_y (kg/cm ²)	f_u (kg/cm ²)	ϵ_u (%)
Longitudinal Reinf.	Deformed Bar 13mm dia.	4120	6116	17.5
Lateral Reinf.	Deformed Bar 6mm dia.	3211	4711	21.9
	High Strength Bar ϕ 5mm	8490	9290	13.1
	Ultra-High Strength Bar ϕ 5.1mm	13882	14315	7.5

f_y : Yield strength of steel bars
 f_u : Ultimate strength of steel bars
 ϵ_u : Ultimate Strain

Table 4 Results of Column Test

Specimen No.	p_o (P/BD) *1	fc' *1	η_o $\frac{p_o}{fc'}$	Yielding of Longit. Reinf. *4 *5		Failure Mode *6	Maximum Strength *4		
				V *2	R *3		V_{max} *2	V_{max} *1	R *3
1	210	680	0.31	28.2	5.0	F	34.0	69.8	10.0
2	240	861	0.28	32.3	5.0	F	36.1	74.1	7.6
3	211	353	0.60	21.1	3.9	FC	22.1	45.4	7.5
4	386	680	0.57	19.2	2.1	FC	37.2	76.4	7.5
5	386	680	0.57	21.4	2.2	FC	36.5	74.9	7.7
6	386	680	0.57	25.1	3.0	FC	36.1	74.1	6.3
7	440	861	0.51	27.1	2.6	FC	35.8	73.5	5.0
8	440	861	0.51	31.0	3.4	FC	38.0	78.0	5.0

p_o : Compressive stress fc' : Measured compressive concrete strength
P : Axial load B : Column width D : Column depth
V : Shear force R : Interstory drift
*1 : kg/cm² *2 : ton *3 : /1000rad. *4 : Values of positive loading
*5 : Values at compression yielding.
*6 : F: Flexural failure FC: Flexural compression failure

Table 5 Details of Short Span Beam Test Specimens

Specimen	1	2	3	4	5	6	7	8	9	10
Cross Section	20 × 30 cm									
Shear Span Ratio	1.5									
Main Bar	7 - D 16							5 - D 16		
Tension Reinf. Ratio	2.71 %							1.86 %		
Transverse Reinf. Ratio P_w (%)	0.76	0.71	1.06	0.78	0.71	0.78	0.71	1.58	0.79	1.58
Spacing of Transverse Reinf. (mm)	50	55	60	50	55	50	55	40	80	40
Yield Strength of Transverse Reinf. f_{yh} (kg/cm ²)	8054	13860	3068	8054	13860	8054	13860	3068	3068	3068
Nominal Shear Stress v_{mu} (kg/cm ²)	65.3							46.6		
Measured Concrete Strength fc' (kg/cm ²)	429	415	621	629	650	840	816	430	407	616
v_{mu} / fc'	0.152	0.157	0.105	0.104	0.101	0.078	0.080	0.108	0.114	0.076
$P_w \cdot f_{yh}$ (kg/cm)	66.2	98.6	32.3	66.2	98.6	66.2	98.6	48.1	24.0	48.1
$P_w \cdot f_{yh} / fc'$	0.154	0.238	0.052	0.105	0.152	0.079	0.121	0.112	0.059	0.078

Table 6 Mechanical Characteristics of Steel Bars

Type of Steel Bars		f_y (kg/cm ²)	f_u (kg/cm ²)	$E_s (\times 10^4)$ kg/cm ²	ϵ_u (%)
Longitudinal Reinf.	Deformed Bar 16mm dia.	4106	6225	1.95	17.7
	Deformed Bar 6mm dia.	3068	5026	1.76	30.2
	High Strength Bar ϕ 5mm	8054	8957	2.05	12.7
	Ultra-High Strength Bar ϕ 5.1mm	13860	14736	2.05	8.5

f_y : Yield strength of steel bars
 f_u : Ultimate strength of steel bars
 E_s : Elastic modulus of steel bars
 ϵ_u : Ultimate strain

Table 7 Results of Short Span Beam Test

Specimen No.	Yielding of Longitudinal Reinforcement		Ultimate Disp. Angle #1 Ru (10 ⁻³ rad.)	Failure Mode #2	Maximum Strength			
	V (ton)	R (10 ⁻³ rad.)			Measured		Calculated	
			V (ton)	R (10 ⁻³ rad.)	Vcal1 (ton)	Vcal2 (ton)		
1	26.1 -26.6	7.01 -6.27	57.7	F S	32.2 -30.7	42.3 -25.1	29.4 (1.09)	30.7 (1.05)
2	24.5 -23.3	6.14 -5.78	50.3	F S	31.4 -31.0	25.2 -25.0	29.4 (1.07)	30.7 (1.02)
3	25.0 -20.0	4.99 -5.06	48.9	F D S	32.1 -30.0	15.5 -25.3	29.4 (1.09)	31.9 (1.01)
4	24.8 -24.1	6.63 -4.15	50.7	F S	30.9 -31.6	40.1 -21.7	29.4 (1.07)	31.9 (0.99)
5	26.8 -26.2	7.15 -5.05	60.2	F S	31.6 -31.7	40.0 -25.1	29.4 (1.08)	32.0 (0.99)
6	26.2 -26.9	6.05 -6.08	48.8	F S	33.0 -33.3	25.1 -40.2	29.4 (1.13)	32.6 (1.02)
7	25.2 -25.3	6.12 -5.95	53.0	F S	33.0 -33.3	40.1 -40.1	29.4 (1.13)	32.6 (1.02)
8	19.4 -19.4	5.14 -5.11	67.7	F S	24.1 -24.0	25.2 -20.3	21.8 (1.11)	23.3 (1.03)
9	20.1 -19.5	6.49 -5.73	32.5	F B S	23.1 -22.4	15.2 -19.8	21.8 (1.06)	23.2 (1.00)
10	17.9 -20.4	3.85 -4.68	62.5	F S	24.9 -25.1	25.9 -42.6	21.8 (1.15)	23.6 (1.06)

V : Shear force in the beam.
Vcal1 : Shear force calculated by flexural strength using the equation of AIJ code
Vcal2 : Shear force calculated by theory for flexural strength using idealized exponential function stress-strain curve for concrete.
#1: A displacement angle at which 80% of maximum shear force was sustained.
#2: FS : Shear failure at hinge zone after flexural yielding.
FDS: Shear-diagonal tension failure after flexural yielding.
FBS: Bond splitting failure after flexural yielding.
Note) Values in parentheses show ratio of measured maximum strength to calculated ones.

Table 8 Details of Test Subassemblages

Specimen	J4-0	J6-0	J6-1	J6-2	J6-3	J8-0	J8H-0	J8H-3	
Specified Concrete Strength f_c (kg/cm ²)	400	600				800			
C O L U M N	Cross Section	44 × 44 cm							
	Type of Main Bar	D22 ($f_y \approx 4000\text{kg/cm}^2$)				D22 ($f_y \approx 6000\text{kg/cm}^2$)			
	Total Area ratio of Main Bars	2.4% (12 - D22)				2.4% (12 - D22)			
	Tension Reinforcement Ratio	0.88 %							
	Area Ratio of Hoop Reinforcement	0.56 %		0.65 %	0.56%		0.88%		
B e a m	Cross section	30 × 40 cm							
	Type of Main Bar	D22 ($f_y \approx 4000\text{kg/cm}^2$)				D22 ($f_y \approx 6000\text{kg/cm}^2$)			
	Tension Reinforcement Ratio	3.1 % (8 - D22)							
	Area Ratio of Stirrup Reinf.	0.5 %		0.6 %	0.5 %		0.75%		
J O I N T	Nominal Shear Stress v_n (kg/cm ²)	140		170	140		200		
	Area Ratio of Joint Reinf.	0.60 %	0.60 %		0.62 %	2.20% *	0.60 %	3.90% *	
	Remarks	Reinf. by Hoops	Reinf. by Hoops	Reinf. by Hoops Anchor Plates	Reinf. by Hoops Moving Hinge	Reinf. by Plates $t=3.2\text{mm}$	Reinf. by Hoops	Reinf. by Plates $t=5.75\text{mm}$	

* Equivalent Value of Plates

Table 9 Yield Strengths of Steels and Compressive Strengths of Concretes

Specimen	unit (kg/cm ²)							
	J4-0	J6-0	J6-1	J6-2	J6-3	J8-0	J8H-0	J8H-3
Column Main Bar (D22)	4080						5790	
Beam Main Bar (D22)	3930			4080 10596*	4080	3930	5790	
Hoop (Φ 9)	9406							
Stirrup(Φ 6)	8700							
Plate	--	--	--	--	2680	--	--	2880
Concrete Strength**	310	617	635	660	683	791	817	838

** Yield Strength of Steel Bars passing through the joint (0.2% offset)
 ** Average compressive strength of three sealed cylinders (20cm high × 10cm dia.)

Table 10 Results of Beam-Column Joint Test

Specimen	Shear cracking at joint					Maximum Strength					Failure Mode
	V (t)	R (10 ⁻³ rad.)	v _{jc} (kg/cm ²)			V (t)	R (10 ⁻³ rad.)	v _{imax} (kg/cm ²)			
			Exp. ¹⁾	Cal. ²⁾	Exp. Cal.			Exp. ¹⁾	Cal. ²⁾	Exp. Cal.	
J4-0	32.8	4.3	73	61	1.20	59.4	19.9	132	137	0.96	J
J6-0	38.5	4.2	86	75	1.15	-70.6	-49.1	157	137	1.15	B J
J6-1	24.3	2.1	54	76	0.71	68.3	48.6	152	137	1.11	B J
J6-2	32.4	3.1	75	80	0.94	80.3	49.1	185	172	1.08	B
J6-3	-23.8	-2.2	55	81	0.68	68.4	49.8	158	143	1.10	B J
J8-0	42.4	5.0	94	82	1.15	69.1	49.6	153	137	1.12	B J
J8H-0	38.7	4.2	86	82	1.05	90.6	20.0	201	202	1.00	B J
J8H-3	-31.2	-3.3	69	83	0.83	92.3	46.8	205	202	1.01	B J

J : Shear failure in joint B J : Shear failure in joint after beam yielding
 B : Flexural failure at beam end

- 1) $v_i = \frac{\sum Ma}{(1 + \xi) \cdot t_b \cdot j_B \cdot j_c}$, $Ma = V \frac{H}{L} - 1$
 V : Story shear force, H : Span between inflection points in the column.
 L : Span between inflection points in the beam.
 l : Distance between column face and inflection point in the beam.
 ξ : Ratio of beam depth to column clear span.
 j_B, j_c : 7/8 of effective beam depth and column depth, respectively.
 t_b : Column depth at shear cracking and average of column depth and beam depth at maximum strength.
- 2) $v_{jc} = ft \sqrt{1 + p_o / ft}$, $ft = 1.6 \sqrt{fc'}$
 p_o : Axial compressive stress, fc' : Compressive strength of concrete
- 3) Following calculated moment were used. M_{cal.} = 0.9 · at · f · d
 at : Area of beam main bars. f : Yield strength of main bar.
 d : Effective beam depth.

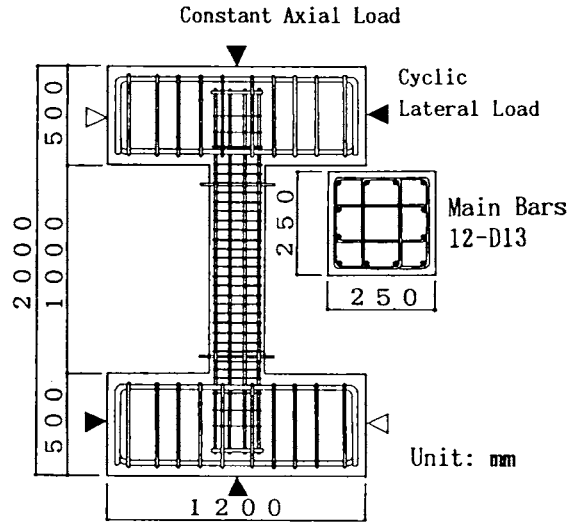


Fig.1 Specimen for Column Test

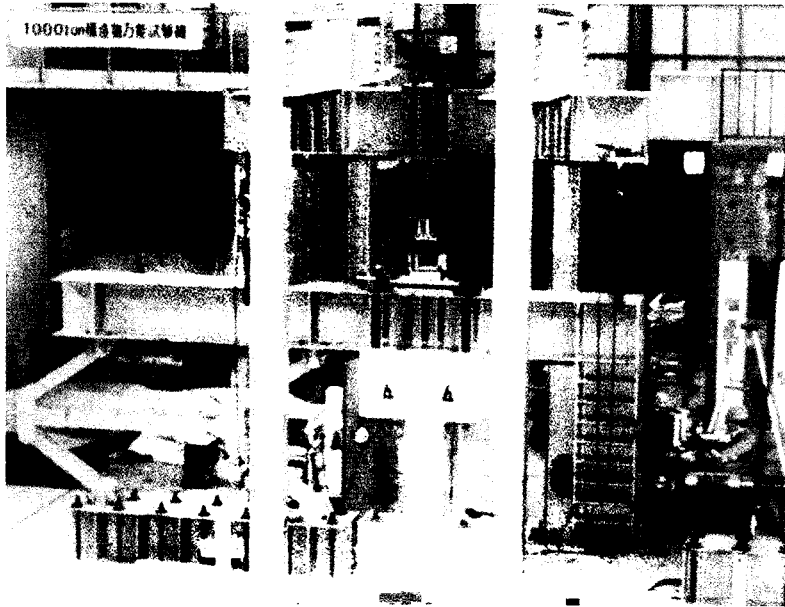


Fig.2 Loading apparatus for Column Test

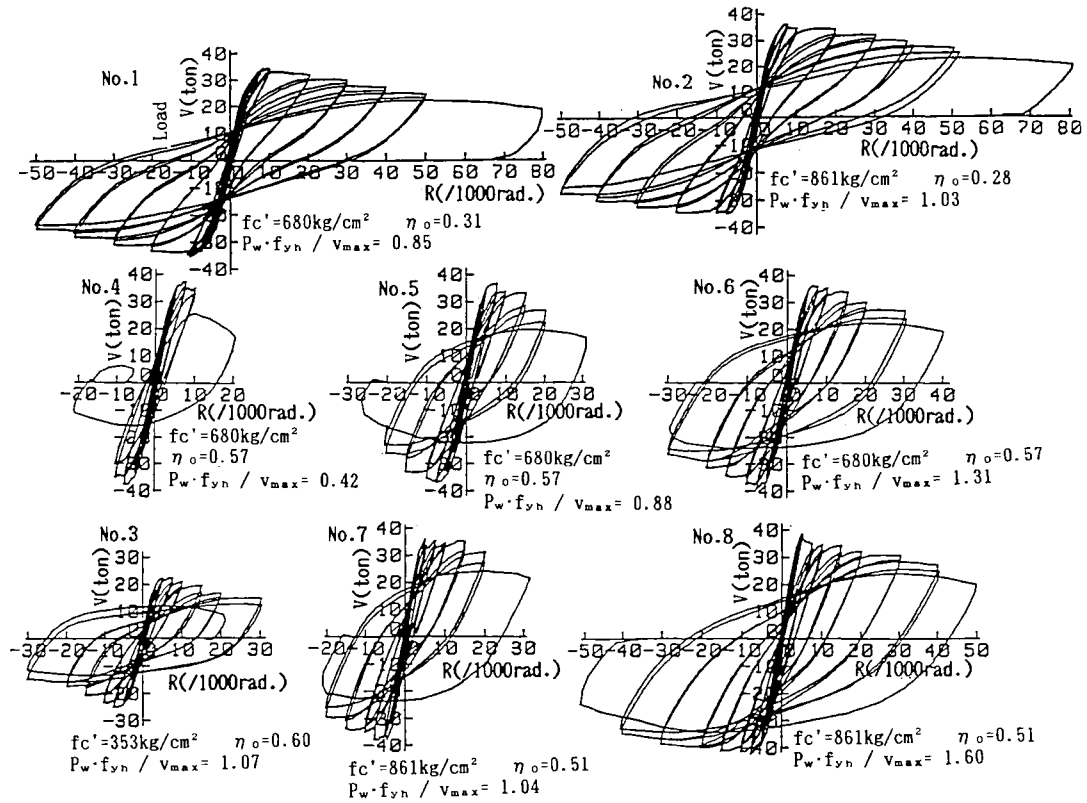


Fig.3 Comparison of Horizontal Load - Interstory Curves

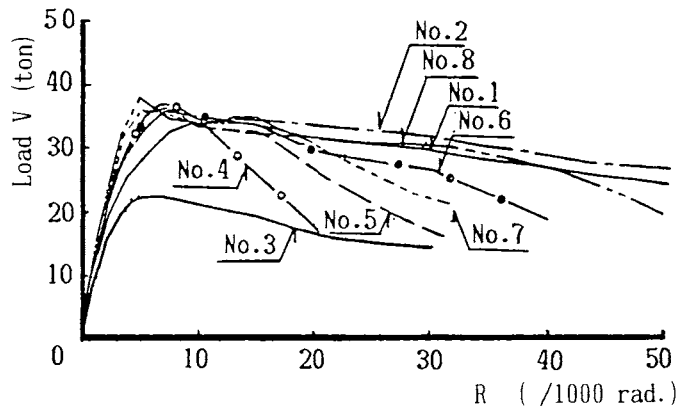


Fig.4 Envelopes of Horizontal Load - Interstory Curves

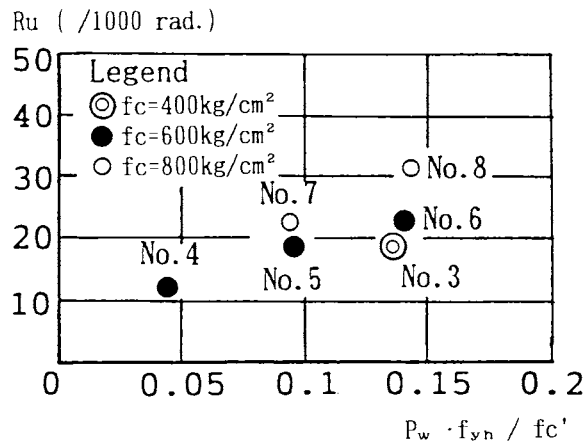
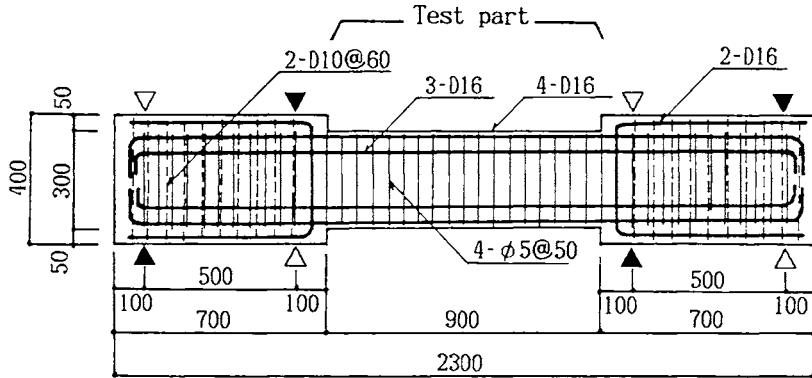
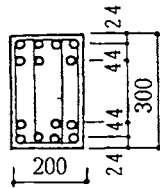


Fig.5 Maximum Ultimate Disp. (R_u) versus the Full Capacity of Lateral Reinf. Normalized by Concrete Strength ($P_w \cdot f_{yh} / f_c'$)



Test part



- Main Bars
7-D16 (SD40)
- Stirrup
(High strength
butt-welded
closed-stirrups)
4-φ5@50

- △ : Positive Loading
- ▲ : Negative Loading

Fig.6 Specimen for Short Span Beam Test

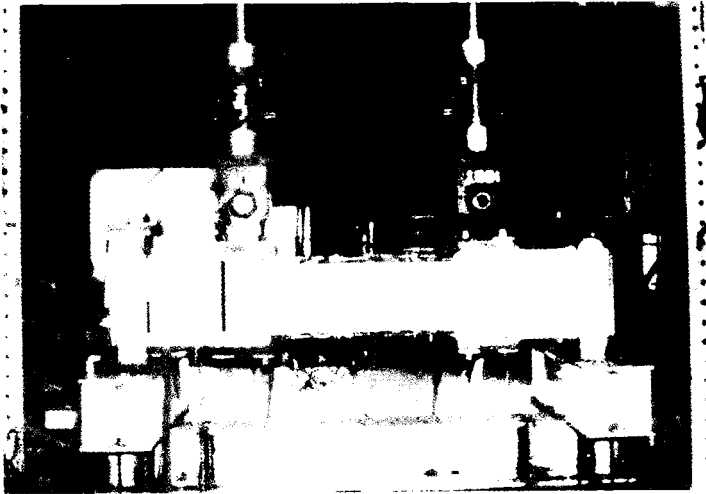


Fig.7 Loading Apparatus for Short Span Beam Test

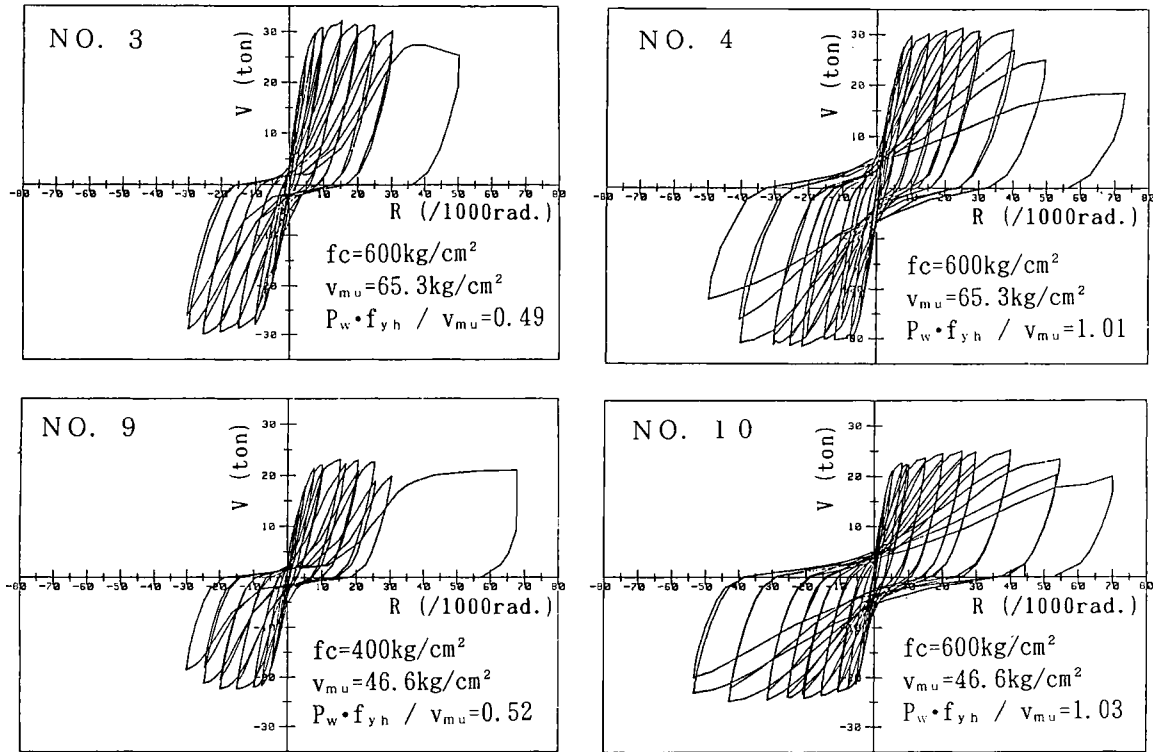


Fig.8 Comparison of Shear Force - Deflection Curves

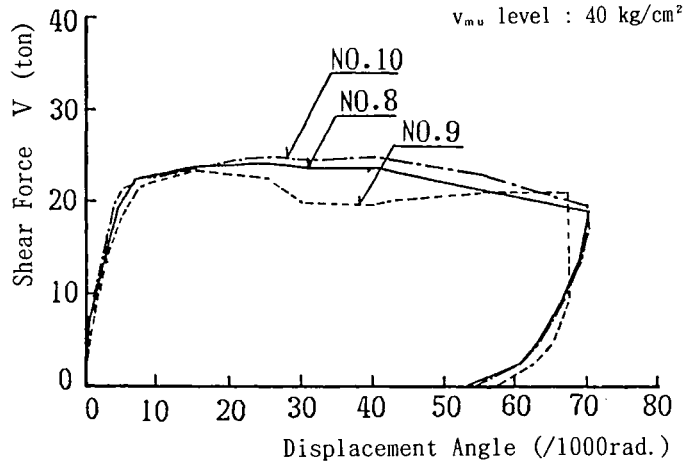
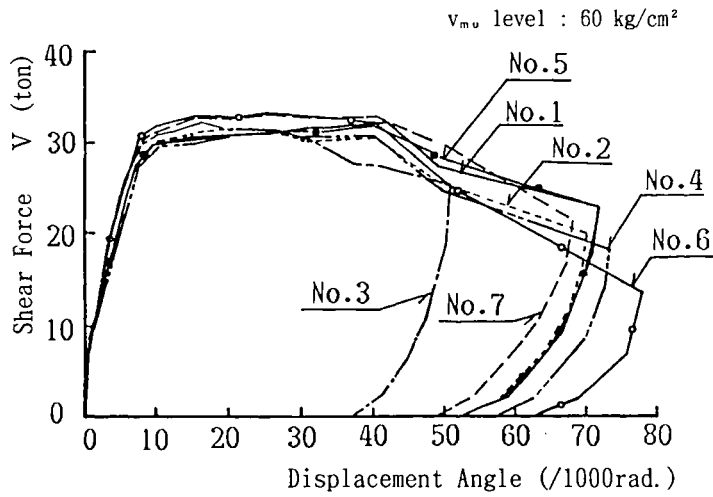


Fig.9 Envelopes of Shear Force - Deflection Curves

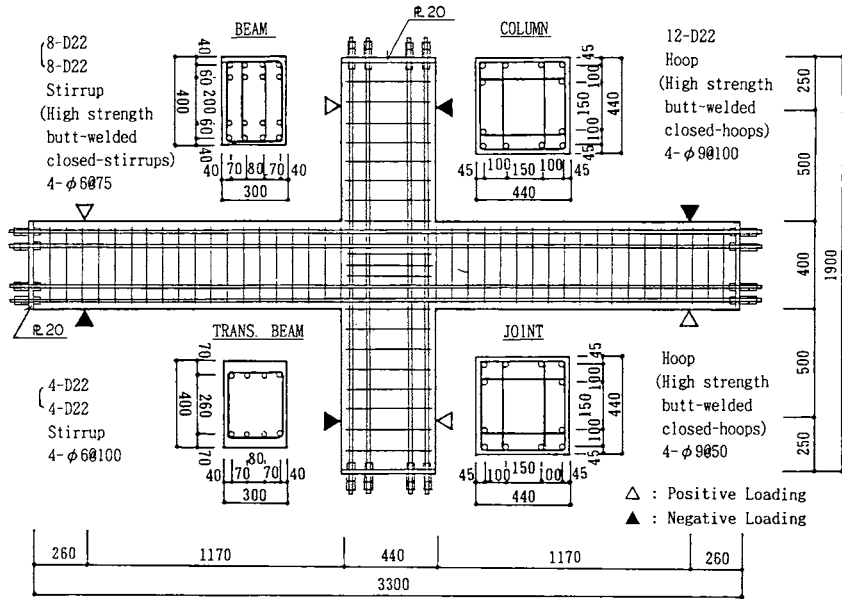


Fig.10 Test Subassemblage (J8-0)

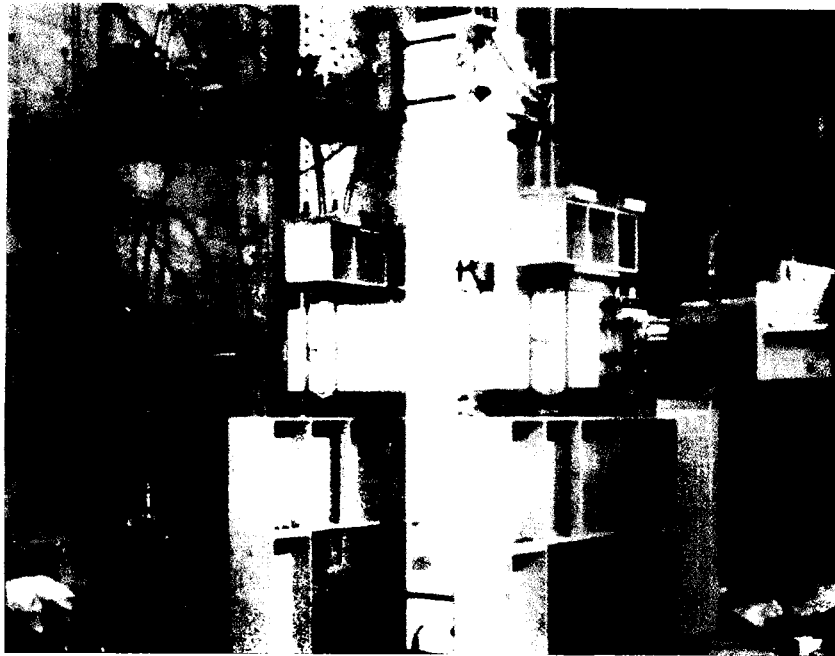


Fig.11 Loading Apparatus for Beam-Column Joint Test

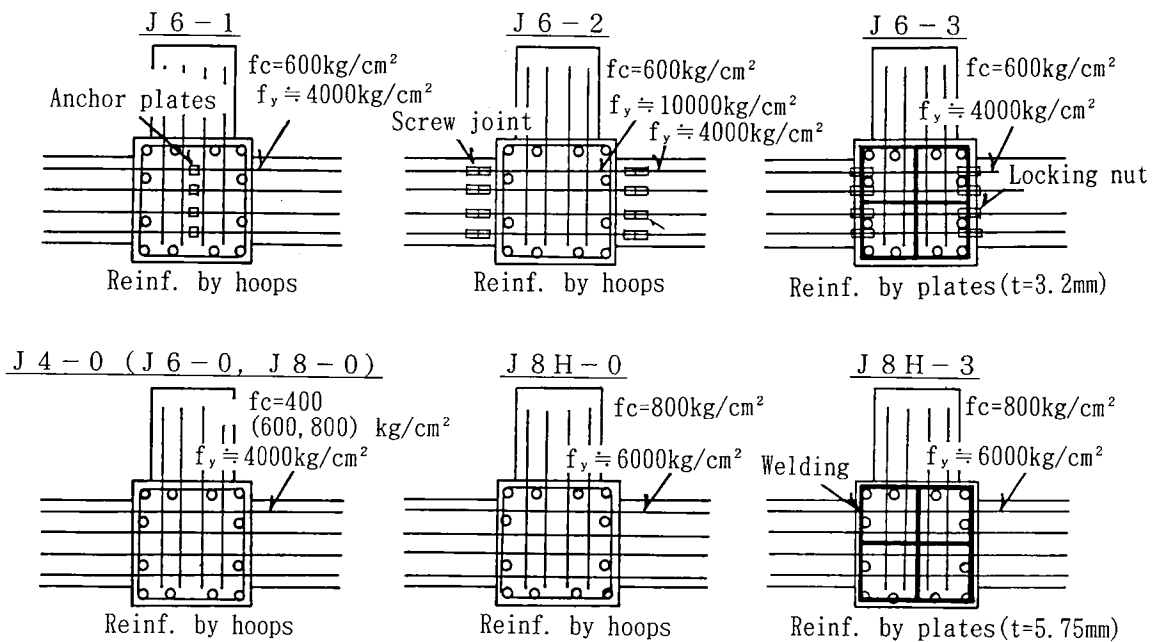


Fig.12 Details of Joint

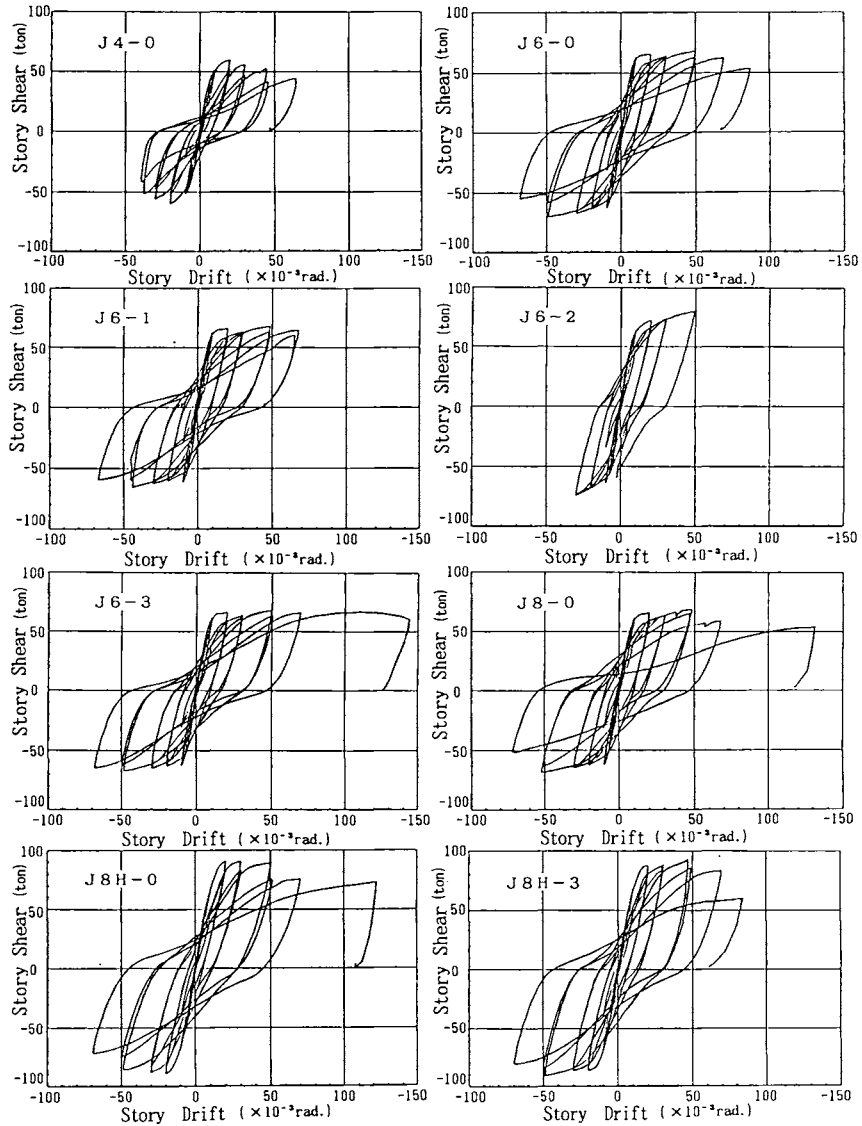
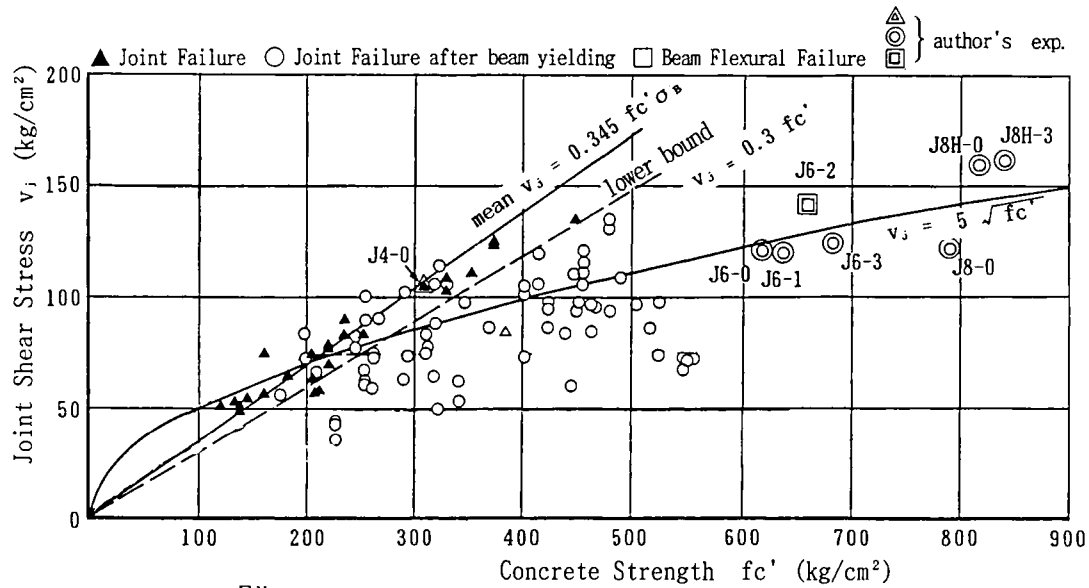


Fig.13 Comparison of Lateral Load - Story Drift Curves



$$v_j = \frac{\sum Ma}{(1 + \xi) \cdot t_p \cdot j_B \cdot D_c}$$

- Ma : Maximum moment in the beam or column adjacent to the joint.
- ξ : Ratio of beam depth to column clear span.
- t_p : Average of column depth and beam depth.
- j_B : 7/8 of effective beam depth .
- D_c : Column depth.

Fig.14 Relationship between the Maximum Joint Shear Stress and the Compressive Strength of Concrete